LaSrVO$_4$: A candidate for the spin-orbital liquid state

Z. L. Dun,[1] V. O. Garlea,[2] C. Yu,[3] Y. Ren,[3] E. S. Choi,[4] H. M. Zhang,[5] S. Dong,[5] and H. D. Zhou[1,4]

[1]*Department of Physics and Astronomy, University of Tennessee, Knoxville, Tennessee 37996-1200, USA*

[2]*Quantum Condensed Matter Division, Oak Ridge National Laboratory, Oak Ridge, Tennessee 37831-6393, USA*

[3]*Advanced Photon Source, Argonne, Argonne National Laboratory, Illinois 60439, USA*

[4]*National High Magnetic Field Laboratory, Florida State University, Tallahassee, Florida 32306-4005, USA*

[5]*Department of Physics, Southeast University, Nanjing 211189, China*

A layered perovskite LaSrVO$_4$ was studied by neutron diffraction, pair distribution function measurement using synchrotron x-ray, susceptibility, and specific heat measurements, and first-principles calculation. The results show (i) a weak structural distortion around 100 K with the existence of orbital fluctuations both above and below it; (ii) the absence of the long range magnetic ordering down to 0.35 K but the appearance of a short range magnetic ordering around 11 K with a T^2 behavior of the specific heat below it. Meanwhile, the calculation based on the density functional theory predicts a magnetic ordered ground state. All facts indicate a melting of the magnetic ordering due to the orbital fluctuations in LaSrVO$_4$, which makes it a rare candidate for the spin-orbital liquid state related to t_{2g} orbitals.

I. INTRODUCTION

The intriguing physical properties related to the orbital ordering transition in $3d$ transitional metal oxides such as perovskites RTiO$_3$ [1,2], RVO$_3$ [3–5], and RMnO$_3$ [6] (R = rare earth elements and Y), and spinels AV$_2$O$_4$ [7–9] (A = Mn, Fe, Zn, Mg, and Cd) have caught a lot of attention during the last several decades. Normally, the orbital ordering transition in these systems is accompanied with structural distortion and long range magnetic ordering (LRMO). Meanwhile, recent evidence reveals that, in some rare systems, the orbital fluctuations due to the frustrated orbital degrees of freedom can efficiently suppress the LRMO and therefore lead to exotic states of matter such as the novel spin-orbital liquid (SOL) state. The studied candidates for SOLs are (i) triangular lattice system LiNiO$_2$ [10,11] and spinel FeSc$_2$O$_4$ [12], in which the geometrically frustrated lattices play the key role for the frustrated orbital degrees of freedom of Ni^{3+} ($3d^7$, $t_{2g}^6 e_g^1$) and Fe^{2+} ($3d^6$, $e_g^3 t_{2g}^3$), and (ii) Ba$_3$CuSb$_2$O$_9$ [13,14] with the honeycomb lattice where the strong spin-orbital entanglements of Cu^{2+} ($3d^9$, $t_{2g}^6 e_g^3$) ions lead to the SOL state. It is noticed that for these three systems, orbital degrees of freedom are all from the e_g orbitals. An orbital liquid state for the t_{2g} orbital of Ti^{3+} ($3d^1$, t_{2g}^1) ions in LaTiO$_3$ [15,16] has been proposed but experimentally it is still under debate [1]. The realization of a SOL state related to t_{2g} orbitals has been a grand challenge.

In this paper, we explore the physical properties of a layered perovskite LaSrVO$_4$. The results suggest a melting of the LRMO due to orbital fluctuations in LaSrVO$_4$, which makes it a rare candidate for the SOL state of t_{2g} orbitals. It is well known that the layered perovskites A_2BO$_4$ with K$_2$NiF$_4$ structure exhibit various intriguing physical phenomena. Examples include the orbital ordering transition in Sr$_2$VO$_4$ [17–19] for V^{4+} ($3d^1$, t_{2g}^1) ions, the low-temperature superconductivity in Sr$_2$RuO$_4$ for Ru^{4+} ($4d^1$) ions [20], and the novel $J_{\text{eff}} = 1/2$ Mott state in Sr$_2$IrO$_4$ with strong spin-orbital coupling for Ir^{4+} ($5d^5$) ions [21]. With La^{3+} doping on the Sr^{2+} sites, La$_{2-x}$Sr$_x$CuO$_4$ [22] exhibits the celebrated high-temperature superconductivity, La$_{2-x}$Sr$_x$MnO$_4$ [23] exhibits complicated

magnetic phase diagram including orbital ordering, charge ordering and spin glass, and La$_{2-x}$Sr$_x$NiO$_4$ [24] exhibits dynamics charge stripes. The reported data on LaSrVO$_4$ [25,26] show that it has the K$_2$NiF$_4$ structure without magnetic ordering down to 5 K. This fact, plus the fact that the V^{3+} ($3d^2$, t_{2g}^2) ions in LaSrVO$_4$ also have the orbital degrees of freedom makes it a promising candidate for the SOL related to t_{2g} orbitals, which deserves detailed exploration.

II. EXPERIMENT

The sample LaSrV$_2$O$_5$ was first prepared by solid state reaction in air of the appropriate mixture of SrCO$_3$, La$_2$O$_3$, and V$_2$O$_5$ at 800 °C for 60 hours. Polycrystalline LaSrVO$_4$ compound was made by reduction of LaSrV$_2$O$_5$ under a 30% H$_2$/Ar flow at 1050 °C for 100 hours, with several grindings of the sample. A Perkin-Elmer TGA-7 thermogravimetric analyzer (TGA) was used to determine the oxygen content of the LaSrVO$_4$ samples from the weight gain on oxidation of the V^{3+} ions to V^{5+} on heating to 700 °C in air. DC and AC magnetic susceptibilities were measured with a Quantum Design DC superconducting quantum interference device (SQUID) magnetometer. The DC susceptibility was measured after cooling in either zero field (ZFC) or in a field (FC) of 2000 Oe. The specific heat was measured with a Quantum Design physical property measurement system (PPMS). The neutron powder diffraction (NPD) measurements were performed on HB2A at Oak Ridge National Laboratory (ORNL) with wavelengths 1.537 Å and 2.41 Å. The pair distribution function (PDF) measurements were carried out at the Advanced Photon Source (APS), beam line 11-ID-C, using 115 keV x rays.

The DFT calculation was performed based on the projected augmented wave (PAW) pseudopotentials using the Vienna *ab initio* simulation package (VASP). The electron-electron interaction is described using the generalized gradient approximation (GGA) and GGA + U method. [27] The effective Hubbard parameter $U_{\text{eff}} = U - J$ is applied on the $3d$ electrons of V. The energy cutoff is 500 eV. The unit cell is

doubling in the *a-b* plane, with four chemical formula units, to host various antiferromagnetic candidates. The Γ-center *k*-point grid is $9 \times 9 \times 4$ in combination with the tetrahedron method.

III. RESULTS AND DISCUSSIONS

Thermogravimetric analysis (TGA) result shows that the as-prepared sample is $LaSrVO_{4.01(1)}$, which is a good insulator at room temperature. The neutron powder diffraction pattern measured at 200 K with wavelength 1.537 Å is shown in Fig. 1(a). The calculated black line is a result of refinement of disordered La/Sr symmetry model $I4/mmm$, in which La and Sr atoms occupy the same Wyck Symb sites 4*e*. The refined lattice parameters are $a = 3.86751(4)$ Å and $c = 12.6337(2)$ Å, consistent with reported data [25,26]. The refinement gives Bragg *R* factor 4.27% and R_f factor 3.06. The structural parameters are listed in Table I. However, neutron data refinement does not exclude the possibility of an ordered La/Sr structure. A refinement with a layered La/Sr arrangement ($P4/mmm$ symmetry) works equally well with Bragg *R* factor 3.8% and R_f factor 4.3 (not shown here). The 200 K and 4 K neutron diffraction patterns measured with wavelength 2.41 Å are shown in Fig. 1(b). Their difference scattering shows no additional Bragg peak nor peak intensity change [Fig. 1(c)].
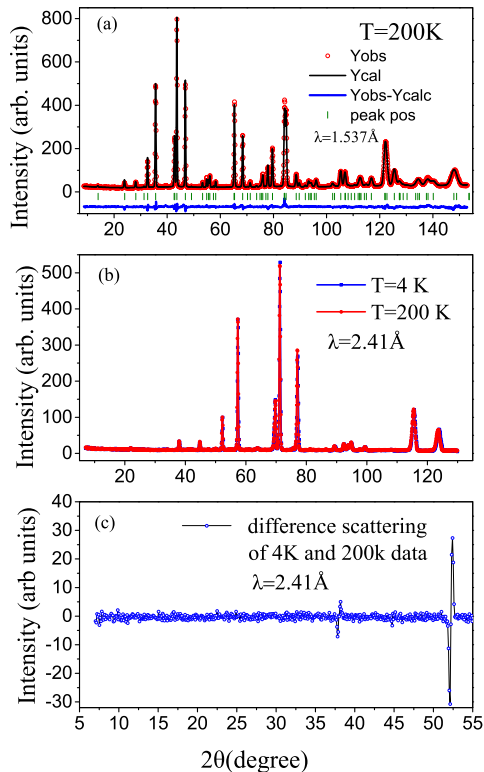
FIG. 1. (Color online) (a) Neutron powder diffraction pattern (open circles) for $LaSrVO_4$ measured at 200 K with wavelength 1.537 Å. The solid line is the refinement with disordered La/Sr lattice space group $I4/mmm$ by using FULLPROF. (b) Comparison between 4 K and 200 K neutron powder diffraction patterns of $LaSrVO_4$ with wavelength 2.41 Å. (c) The difference between 4 K and 200 K data in (b).
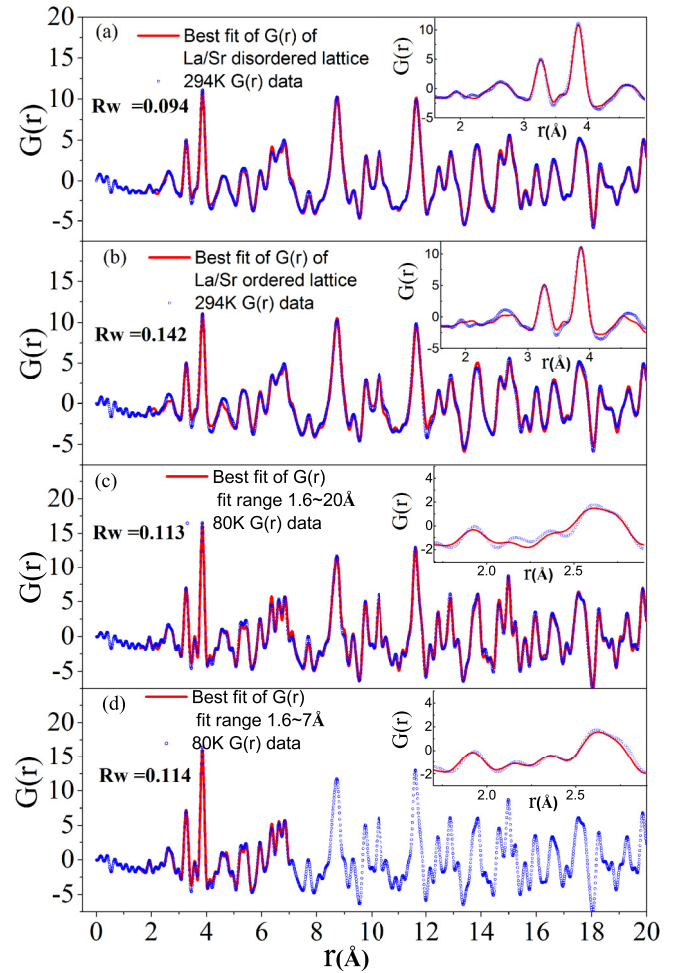
FIG. 2. (Color online) Pair distribution function (PDF) data sets and refinements for (a) 294 K data and best fitting with disordered La/Sr space group $I4/mmm$; (b) 294 K data and best fitting with ordered La/Sr space group $P4/mmm$; (c) 80 K data and best fitting with *r* range 1.6–20 Å; (d) 80 K data and best fitting with *r* range 1.6–7 Å. Both (c) and (d)are fitted with the disordered La/Sr model. For comparison, low-*r* regions $G(r)$ are zoomed as inset plots in each graph.

The only noticeable feature is due to the shift in Bragg peak position as a result of change in lattice parameters.

Details of pair distribution functions (PDFs) measured at 80 K and 294 K and refinements are shown in Fig. 2. Data reduction is carried out using the software PDFGETX2, and fitting and refinements are performed by the program PDFGUI. The room-temperature PDF data set refinement is done in the *r* range 1.6 to 20 Å. The region before the first physical meaningful peak at 1.9 Å is mostly excluded because of the wiggle of $G(r)$. Two modeld are tested: the disordered La/Sr model with $I4/mmm$ symmetry [Fig. 2(a)] and the ordered model of La/Sr layer structure with $P4/mmm$ symmetry [Fig. 2(b)]. Refined parameters include scale factor, Q_{damp}, linear atomic correlation factor, lattice constants, symmetry constrained atomic position, and thermal factors. The final R_w value obtained for the disordered model is 9.4%, better than that for the ordered model of 14.2%. This is also well reflected by the agreement between fitting and data in the low-*r* region as

TABLE I. Crystallographic parameters and selected bond lengths of LaSrVO$_4$ for (a) neutron powder diffraction refinement at 200 K, (b) neutron powder diffraction refinement at 4 K, (c) PDF $G(r)$ refinement at 294 K, and (d) PDF $G(r)$ refinement at 80 K. All refinements are done with La/Sr disordered $I4/mmm$ symmetry.

Refinement	Atom	x	y	z	B_{iso} (Å^2)	Occu.	Refinement	Atom	x	y	z	u_{11} ($=u_{22}$)	u_{33}	Occu.
Neutron	La	0	0	0.35761(8)	0.30(1)	0.5	PDF	La	0	0	0.3575(9)	0.0061(7)	0.0042(2)	0.5
200 K	Sr	0	0	0.35761(8)	0.30(1)	0.5	294 K	Sr	0	0	0.3575(9)	0.0061(7)	0.0042(2)	0.5
(a)	V	0	0	0	0.3	1	(c)	V	0	0	0	0.0055(6)	0.0083(6)	1
	O(1)	0	0	0.1668(1)	0.92(3)	1		O(1)	0	0	0.1658(5)	0.096(4)	0.017(8)	1
	O(2)	0	0.5	0	0.44(2)	1		O(2)	0	0.5	0	0.015(5)	0.057(4)	1

<div align="center">

V-O(1) = 2.108(1) Å 　　　　　　　　　　　　　　V-O(1) = 2.092(0) Å

V-O(2) = 1.9338(1) Å 　　　　　　　　　　　　　V-O(2) = 1.9316(8) Å

$a = b = 3.86751(4)$ Å, 　$c = 12.6337(2)$ Å　　　　　$a = b = 3.8633(6)$ Å, 　$c = 12.606(4)$ Å

$R_{Bragg} = 4.27\%$, $R_f = 3.06$, $\chi^2 = 1.62$ 　　　　　　　　$R_w = 9.4\%$

</div>

Refinement	Atom	x	y	z	B_{iso} (Å^2)	Occu.	Refinement	Atom	x	y	z	u_{11} ($=u_{22}$)	u_{33}	Occu.
Neutron	La	0	0	0.35727(7)	0.29(2)	0.5	PDF	La	0	0	0.3575(6)	0.0029(9)	0.0022(4)	0.5
4 K	Sr	0	0	0.35727(7)	0.29(2)	0.5	80 K	Sr	0	0	0.3575(6)	0.0029(9)	0.0022(4)	0.5
(b)	V	0	0	0	0.3	1	(d)	V	0	0	0	0.0039(9)	0.0048(6)	1
	O(1)	0	0	0.1666(1)	0.81(3)	1		O(1)	0	0	0.1679(1)	0.095(4)	0.016(3)	1
	O(2)	0	0.5	0	0.35(2)	1		O(2)	0	0.5	0	0.014(7)	0.041(4)	1

<div align="center">

V-O(1) = 2.104(1) Å 　　　　　　　　　　　　　　V-O(1) = 2.117(0) Å

V-O(2) = 1.9308(1) Å 　　　　　　　　　　　　　V-O(2) = 1.926(5) Å

$a = b = 3.86176(4)$ Å, 　$c = 12.6311(2)$ Å　　　　　$a = b = 3.8530(4)$ Å, 　$c = 12.5937(0)$ Å

$R_{Bragg} = 6.28\%$, 　$R_f = 7.04$, $\chi^2 = 2.47$ 　　　　　　$R_w = 11.3\%$

</div>

shown in insets of Figs. 2(a) and 2(b): the disordered model fits peak position and intensity well while the ordered model does not. Therefore, although neutron scattering does not exclude the La/Sr ordering, we prefer to accept the disordered structure of La/Sr based on the PDF results. The full region refinements of PDF data give structural parameters (Table I) similar to those obtained from the NPD data refinements.

Although the structure of LaSrVO$_4$ retains the $I4/mmm$ symmetry down to 4 K, the c axis expands with decreasing temperature [Fig. 3(a)] below 100 K. In order to extract the relative change in lattice constant c, c is fit to a suitable polynomial above 100 K. Within this intermediate temperature region (100–200 K), the temperature dependencies of the lattice parameters can be fit well to a T^2 behavior [solid lines in Figs. 3(a) and 3(b)], which can be described as

$$c_B(T) = c_0(1 + AT^2),\qquad(1)$$

with $c_0 = 12.6288$ Å and $A = 8.49 \times 10^{-8}$ K^{-2}. Then we extend this fitting, c_B, down to 4 K and take it as the lattice background below 100 K. Accordingly, the relative change of c below 100 K is calculated as $\Delta c = (c - c_B)/c_B$, as shown in the inset of Fig. 3(a). The similar fitting is also performed for the lattice parameter a [Fig. 3(b)]. Although the raw data show no obvious anomaly, the a shows a gradual shrink with decreasing temperature below 100 K, comparing to the calculated lattice background a_B. The experimental c/a ratio is shown in Fig. 3(c). By comparing to the fitting value c_B/a_B (the solid line), the c/a ratio shows an expansion below 100 K. The experimental value of the volume (V) shows a shrink below 100 K by comparing to the fitting value $V_B = a_B^2 \times c_B$. $\Delta V = (V - V_B)/V_B$ is shown in the inser of Fig. 3(d).

These results show a structural distortion without structural phase change around 100 K for LaSrVO$_4$. Our former studies on Sr$_2$VO$_4$, with the same structure but V^{4+} magnetic ions, also

show a structural distortion with the expansion of c and shrink of a below 100 K. For comparison, the Δc, Δa, c/a, and ΔV for Sr$_2$VO$_4$, calculated with the same method described above for LaSrVO$_4$, are shown in Fig. 3. Although for both samples the structural distortion occurs around similar temperatures, the obvious differences are that the changes of c, a, and c/a below 100 K are much smaller and more gradual for LaSrVO$_4$ compared to those larger and abrupt changes for Sr$_2$VO$_4$. For example, the Δc and Δa at 50 K for LaSrVO$_4$ are around
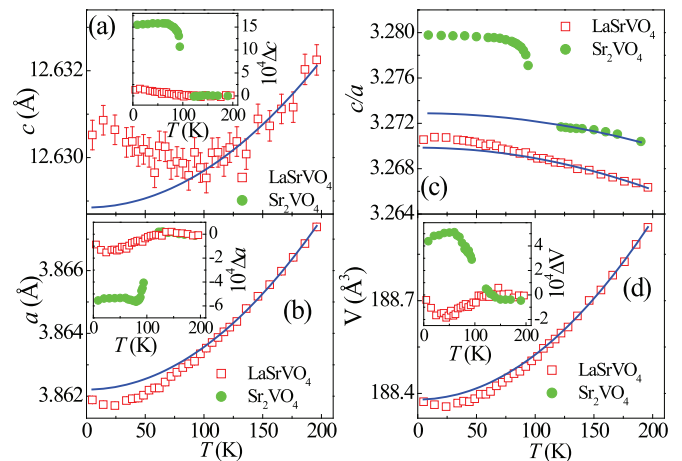
FIG. 3. (Color online) (a) Temperature dependencies of the lattice parameters c (a), a (b) for LaSrVO$_4$, c/a ratio (c) for LaSrVO$_4$ and Sr$_2$VO$_4$, and volume (V) (d) for LaSrVO$_4$. Temperature dependencies of Δc [inset of (a)], Δa [inset of (b)], and ΔV [inset of (d)] for LaSrVO$_4$ and Sr$_2$VO$_4$. Open circles are experimental data. The solid lines in (a) and (b) are fittings using Eq. (1). The solid lines in (c) and (d) are calculations based on the fitted a_B and c_B as described in the text. In (b), the error bar is smaller than the data points.

1×10^{-4} and -2×10^{-4}, respectively, but they are 15×10^{-4} and -5×10^{-4} for Sr_2VO_4, respectively.

The structural distortion, with an abruptly jump of c/a around 100 K for Sr_2VO_4, has been attributed to an orbital ordering transition with the increasing occupancy of the d_{xz}/d_{yz} orbitals of the $V^{4+}(3d^1)$ electrons [17,18]. By replacing one Sr^{2+} with one La^{3+} ion, the valence of vanadium changes to $3+$ in $LaSrVO_4$, which still has t_{2g} orbital degrees of freedom with the $3d^2$ electronic configuration to lead to a possible orbital ordering transition. Actually, the orbital ordering transition for V^{3+} orbitals in perovskite RVO_3 and spinel AV_2O_4 has received considerable attention. Accordingly, the structural distortion for $LaSrVO_4$ observed here, which occurs around 100 K as that for Sr_2VO_4 does, is possibly related to the orbital ordering transition of V^{3+} ions. However, this subtle and gradual structural distortion for $LaSrVO_4$ also suggests that this transition is not a completed long range orbital ordering as that for Sr_2VO_4, which leads to large and abrupt structural distortions. The short range orbital ordering or orbital fluctuations may exist in $LaSrVO_4$.

In $LaSrBO_4$, the $3d$ orbitals are split into t_{2g} and e_g orbitals, and the t_{2g} orbitals are further split into the xy orbital and degenerate xz and yz orbitals due to the tetragonal elongation of the oxygen octahedra along the c axis. This elongation normally leads to two long V-O1 bonds along the c axis and four short V-O2 bonds in the ab plane for BO_6 octahedra. For $LaSrBO_4$ (B = Cr, Fe, Co) [28–30], in which the magnetic B^{3+} ions have no further orbital degrees of freedom or are not Jahn-Teller (JT) active, their elongations represented by the ratio of V-O1 and V-O2 bond lengths are all around $l_{V-O1}/l_{V-O2} \approx 1.10$. On the other hand, for $LaSrMnO_4$ [23] and $LaSrCuO_4$ [31], in which the Mn^{3+} ($3d^4$, $t_{2g}^3 e_g^1$) and Cu^{3+} ($3d^8$, $t_{2g}^6 e_g^2$) ions both have further orbital degrees of freedom or are JT active, the increased occupancy of the out plane e_g ($d_{3z^2-r^2}$) orbital is expected to lead to even larger tetragonal elongation along the c axis. Indeed, for $LaSrMnO_4$ and $LaSrCuO_4$ with JT active ions the elongation shows larger l_{V-O1}/l_{V-O2} ratios as 1.20 and 1.18, respectively. Another similar case is Sr_2VO_4 with JT active V^{3+} ($3d^1$, t_{2g}^1); its increased occupancy of d_{xz} and d_{yz} orbitals leads to larger elongation of the octahedral sites with further expanded c axis [17]. Therefore, in $LaSrBO_4$ the larger l_{V-O1}/l_{V-O2} ratio (> 1.10) is a good indication for the existence of JT distortion to further elongate the V-O1 bonds. For $LaSrVO_4$, the average crystallographic structure obtained from the NPD pattern at 200 K yields $l_{V-O1}/l_{V-O2} = (2.11 \text{ Å})/(1.93 \text{ Å}) = 1.09$, which indicates that there is no obvious JT distortion for VO_6 octahedra from the view of the average structure, although V^{3+} ions are expected to be JT active.

However, the low-r region of the experimental pair distribution function (PDF) data at 294 K [Fig. 4(a)] shows that the V-O1 and V-O2 bonds lengths are 2.184(4) Å and 1.934(7) Å, respectively, which leads to the ratio as 1.13. This larger ratio due to the larger V-O1 bond length shows that the JT distortion of VO_6 octahedra exists locally in $LaSrVO_4$ at room temperature. Moreover, the PDF at 294 K and 80 K were refined to the data over different ranges of r. In general, fits confined to low-r region will yield the local JT distorted structure while the fits over wider ranges of r will gradually
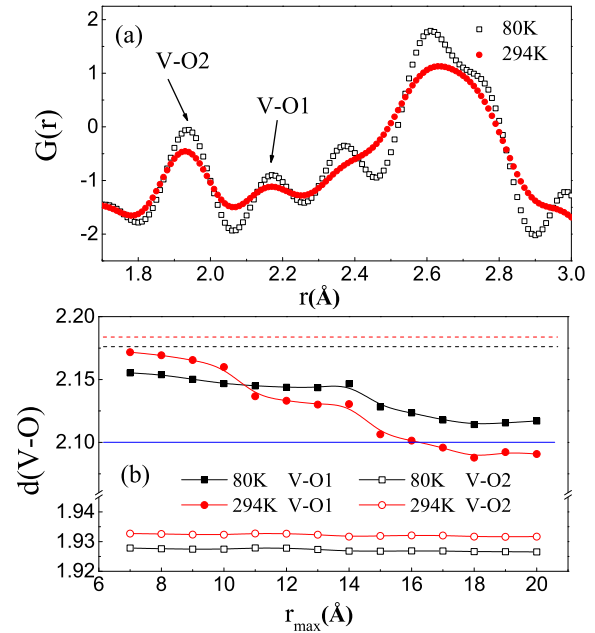
FIG. 4. (Color online) (a) Low-r region of the experimental PDF for $LaSrVO_4$ at 80 K and 294 K. The V-O1 and V-O2 peaks are pointed out by arrows. (b) V-O1 and V-O2 bond lengths from the refined structure model as a function of fitting range r_{max} at 294 K and 80 K (error bar is smaller than the data points). The dash lines indicate the V-O1 bond length extracted from first two $G(r)$ peaks for 294 K and 80 K shown in (a); the solid line indicates V-O1 bond length from the neutron refinement at 200 K.

cross over to the average crystallographic structure. This is reflected by comparison between fittings of fit ranges 1.6–20 Å [Fig. 2(c)] and 1.6–7 Å [Fig. 2(d)] of the 80 K PDF data set. Although they gives similar R_w values, fitting of $G(r)$ for 1.6–7 Å agrees better than that of 1.6–20 Å in the low-r region, where local JT distortion dominates. Accordingly, the V-O1 distance gradually increases from 2.117(0) Å to 2.155(3) Å while the fit range decreases from 1.6–20 Å to 1.6–7 Å. As shown in Fig. 4(b), when comparing the refined V-O bond lengths as a function of the fit range, the V-O2 bond length barely changes, while the V-O1 bond length (or the distortion) approaches the value of peak position in Fig. 4(a) in the small-r region and falls off smoothly as the fit range is extended to higher r until it approaches the smaller crystallographically refined value. This behavior is actually a characteristic feature for the presence of local ordered clusters of JT distorted VO_6 octahedra, which implies the existence of the short range orbital ordering or orbital fluctuations. Similar behaviors have been observed and discussed in $LaMnO_3$ [32]. Our analysis of the 80 K PDF data leads to similar results as that of 294 K data [Fig. 4(b)] but with a more gradual change of V-O1 bond length, which reveals that the local JT distortion forms a larger cluster size but still fails to propagate to a long range orbital ordering state.

The susceptibility (χ, Fig. 5) and specific heat (C_p, Fig. 6) were also measured for $LaSrVO_4$. As shown in Fig. 5(a), $1/\chi$ deviates from a linear behavior below 150 K, but shows no signature for magnetic transition around 100 K. Then, around $T_f = 11$ K, χ exhibits a broad peak with obvious ZFC and
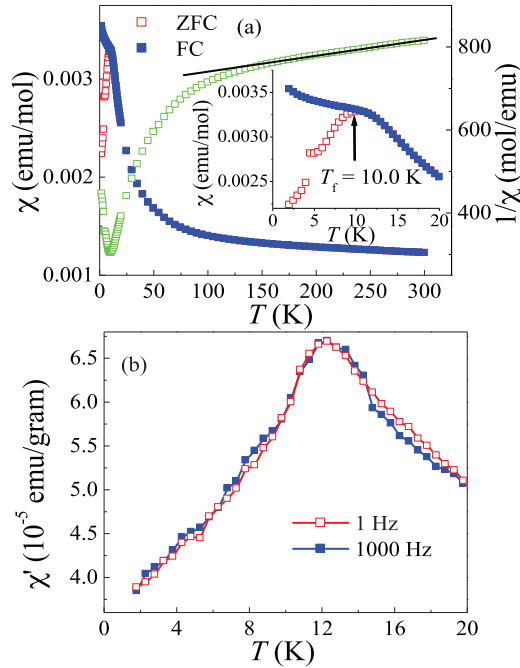
FIG. 5. (Color online) Temperature dependencies of DC susceptibility χ and its inverse (a) and the real part of the AC susceptibility, χ', for LaSrVO$_4$. Inset of (a): The enlargement of χ below 20 K.

FIG. 6. (Color online) Temperature dependencies of specific heat, C_P (a) and the magnetic specific heat, C_{mag} at 0 T (b) for LaSrVO$_4$. In (b) the open squares are experimental data and the solid line is the fitting as described in the text. Insert of (b): The calculated entropy variation between 1 and 30 K.

FC divergence. The further AC susceptibility measurements also exhibit a peak around 12 K without frequency dependence [Fig. 5(b)]. By subtracting the lattice contribution (the specific heat measured for the isostructural and nonmagnetic LaSrGaO$_4$), LaSrVO4 exhibits magnetic contribution of the specific heat (C_{mag}) below 30 K [Fig. 6(a)]. The main features of C_{mag}/T as plotted in Fig. 6(b) are (i) a broad peak around 11 K, which should be related to the susceptibility peak; (ii) a sharp increase below 1 K, which could be related to the nuclear Schottky anomaly for V ions at low temperatures as observed for other V compounds [33]; (iii) the specific heat does not change at 9 T besides the small shift of the 11 K feature; (iv) the magnetic entropy calculated by integrating C_{mag}/T between 1 K and 30 K yields an entropy variation of 0.37 J/mol K [inset of Fig. 6(b)], which is just 4.1% of $R\ln(3)$ for a $S = 1$ system, where R is the gas constant; (v) C_{mag} follows a T^2 behavior between 1 K and 9 K.

The ZFC and FC divergence of the DC susceptibility, the peak of the AC susceptibility, the small magnetic entropy variation, and the unchanged NPD pattern intensity at 4 K all suggest that the anomaly around 11 K is not a LRMO but a kind of short range magnetic ordering. The disappearance of a LRMO down to 0.35 K makes LaSrVO$_4$ distinct from other orbital ordering systems with V^{3+} ions. For examples, in RVO$_3$ and AV$_2$O$_4$, the long range orbital ordering transition is always accompanied by LRMOs. In isostructural Sr$_2$VO$_4$, a LRMO also occurs simultaneously around 100 K with the structural distortion [17]. This feature of LaSrVO$_4$ also differentiates it from other LaSrBO_4.LaSrCrO$_4$ [28], LaSrMnO$_4$ [23], LaSrFeO$_4$ [29], and LaSrCoO$_4$ [30] show LRMO, either antiferromagnetic or ferromagnetic, at 242, 125, 380, and 90 K, respectively.
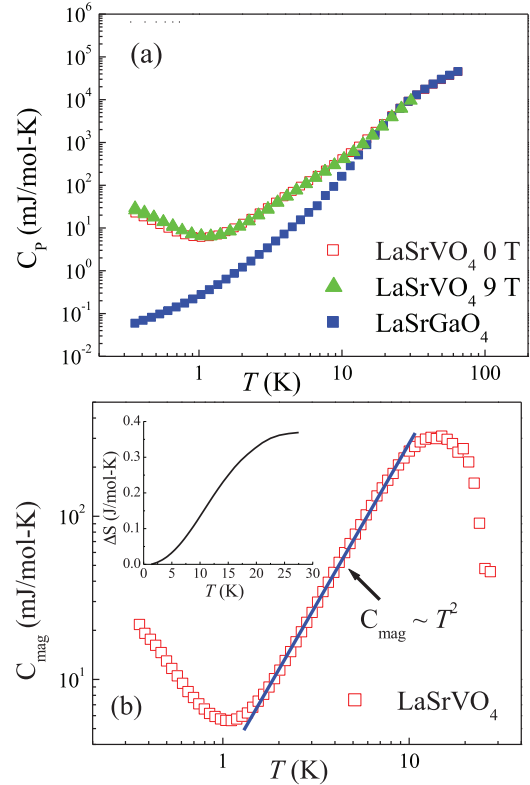
Furthermore, a density functional theory (DFT) calculation was performed using the Vienna *ab initio* simulation package (VASP) [27,34,35] for a preliminary comparison with the experimental observation. The experimental crystal structure was adopted in the calculation. Several site arrangements of La and Sr ions were tested. The A-site configuration with the lowest energy is shown in Fig. 7(a). With this configuration, the magnetic ground state changes from the A-type antiferromagnetic (A-AFM) one ($U_{eff} \leqslant 1.5$ eV) to the G-type antiferromagnetic (G-AFM) one ($U_{eff} \geqslant 2$ eV), as shown in Fig. 7(b). The local moments are calculated using the Wigner-Seitz sphere of V as specified by VASP, which is quite large (1.3–1.8 μ_B per V) as shown in Fig. 7(c). Both the ferromagnetic (FM) and A-AFM phases are metallic while the G-AFM state is insulating when $U_{eff} \geqslant 2$ eV, as shown in Fig. 4(d). Since LaSrVO$_4$ is an insulator, the projected density of states (PDOS) of V's 3d orbitals (the G-AFM state at $U_{eff} = 2.5$ eV) are calculated in Fig. 7(e). The occupied bands near the Fermi levels are contributed by two degenerated localized t_{2g} orbitals: d_{xz} and d_{yz}, as expected from the Jahn-Teller splitting. The in-plane d_{xy} orbitals are higher in energy and are empty. Due to the two-dimensional structure, the bandwidths for the d_{xz} and d_{yz} bands are very narrow, in contrast to the wide xy band.

Although the PDF refinements support the La/Sr site-disorder structure, site- "ordered" structures have to be specified in the DFT calculations. To simulate the disorder
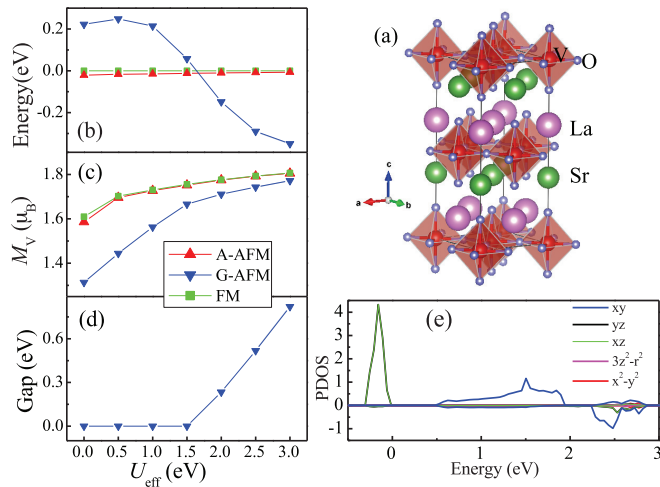
FIG. 7. (Color online) Results of the DFT calculation. (a) The crystal structure with the lowest energy in the DFT calculation. (b) Energies for different magnetic states. The FM state is taken as the reference. (c) Local magnetic moments. (d) Band gap at the Fermi level for the G-AFM phase while both the FM and A-AFM are always metallic. (b)–(d) are presented as a function of the effective Hubbard U_{eff}. (e) PDOS of V's $3d$ orbitals. The G-AFM state is used at $U_{\text{eff}} = 2.5$ eV.

effect, besides the structure shown in Fig. 7(d), many other site arrangements of La and Sr ions were tested. For most configurations, the G-AFM insulating phase is the ground state at a proper U_{eff}, although the detail value of U_{eff} may be shifted a little higher or lower.

While the DFT calculation confirms the Jahn-Teller splitting, it predicts a ground state with the LRMO which has not been observed from our presented studies. Then all facts— (i) LaSrVO$_4$ shows a very weak structural distortion around 100 K indicating a noncompleted orbital ordering transition; (ii) the PDF results show the existence of orbital fluctuations above and below 100 K; (iii) other LaSrBO_4 show a LRMO ground state; and (iv) the orbital fluctuation effect was not taken into account in the DFT calculation—suggest that the orbital fluctuations play an important role in melting the LRMO in LaSrVO$_4$ and it could be a rare example of SOL for t_{2g} orbitals. Recently, theoretical studies on another orbital ordering system, KCuF$_3$, with perovskite structure similar that of LaSrVO$_4$, have proposed that the frustrated orbital degrees of freedom on a square lattice due to the strong spin-orbital entanglements can lead to various magnetic phases including

nonmagnetic and nonorbital ordered SOL state [36–38]. Experimentally, the enhanced orbital fluctuations in KCuF$_3$ under high pressure suppress the magnetic ordering and lead to a quantum spin liquid state [39]. Our former studies on Sr$_2$VO$_4$ also showed that the high pressure can enhance the orbital fluctuations, which suppresses the magnetic ordering around 100 K [40].

Finally, it is noteworthy that the frequency-independent AC susceptibility peak and T^2 behavior of C$_{\text{mag}}$ below 10 K exclude the possibility of a spin-glass transition, which typically should show frequency dependence and linear-T behavior of specific heat [41]. The unchanged specific heat at 9 T, which is on the same energy scale of the possible magnetic transition (11 K), further suggests that this transition is not a typical transition simply originating from magnetism. Actually this T^2 behavior of specific heat is very similar to those of the studied SOL candidates LiNiO$_2$ [10] and FeSc$_2$O$_4$ [12], both of which show a $T^{2.5}$ behavior of specific heat at low temperatures. This further supports that LaSrVO$_4$ potentially is a SOL.

IV. CONCLUSION

In summary, LaSrVO$_4$ shows a weak structural distortion around 100 K with the existence of orbital fluctuations both above and below it. While the DFT calculation predicts a ground state with LRMO and other LaSrAO_4 exhibit magnetic orderings, LaSrVO$_4$ does not but shows a short range magnetic ordering around 11 K with a T^2 behavior of C$_{\text{mag}}$ below it. These facts show that the melting of the magnetic ordering in LaSrVO$_4$ is strongly correlated to the orbital fluctuations, which makes it a rare candidate for SOL related to t_{2g} orbitals. Further studies on this intriguing new system for the SOL state will be able to shed light on the nature of the strong correlation of spin and orbital in exotic magnetic states.

[1] J. G. Cheng, Y. Sui, J. S. Zhou, J. B. Goodenough, and W. H. Su, Phys. Rev. Lett. **101**, 087205 (2008).

[2] G. Khaliullin, Prog. Theor. Phys. Suppl. **160**, 155 (2005).

[3] C. Ulrich, G. Khaliullin, J. Sirker, M. Reehuis, M. Ohl, S. Miyasaka, Y. Tokura, and B. Keimer, Phys. Rev. Lett. **91**, 257202 (2003).

[4] J. Q. Yan, J. S. Zhou, and J. B. Goodenough, Phys. Rev. Lett. **93**, 235901 (2004).

[5] Y. Ren, T. T. M. Palstra, D. I. Khomskii, E. Pellegrin, A. A. Nugroho, A. A. Menovsky, and G. A. Sawatzky, Nature (London) **396**, 441 (1998).

[6] Y. Tokura and N. Nagaosa, Science **288**, 462 (2000).

[7] S. H. Lee, H. Takagi, D. Louca, M. Matsuda, S. Ji, H. Ueda, Y. Ueda, T. Katsufuji, J. H. Chung, S. Park, S. W. Cheong, and C. Broholm, J. Phys. Soc. Jpn. **79**, 011004 (2010).

[8] A. Kismarahardja, J. S. Brooks, A. Kiswandhi, K. Matsubayashi, R. Yamanaka, Y. Uwatoko, J. Whalen, T. Siegrist, and H. D. Zhou, Phys. Rev. Lett. **106**, 056602 (2011).

[9] Y. Kato, G. W. Chern, K. A. Al-Hassanieh, N. B. Perkins, and C. D. Batista, Phys. Rev. Lett. **108**, 247215 (2012).

[10] Y. Kitaoka, T. Kobayashi, A. Koda, H. Wakabayashi, Y. Niino, H. Yamakage, S. Taguchi, K. Amaya, K. Yamaura, M. Takano, A. Hirano, and R. Kanno, J. Phys. Soc. Jpn. **67**, 3703 (1998).

[11] F. Reynaud, D. Mertz, F. Celestini, J. M. Debierre, A. M. Ghorayeb, P. Simon, A. Stepanov, J. Voiron, and C. Delmas, Phys. Rev. Lett. **86**, 3638 (2001).

[12] V. Fritsch, J. Hemberger, N. Büttgen, E. W. Scheidt, H.-A. Krug von Nidda, A. Loidl, and V. Tsurkan, Phys. Rev. Lett. **92**, 116401 (2004).

[13] Y. Ishiguro, K. Kimura, S. Nakatsuji, S. Tsutsui, A. Q. R. Baron, T. Kimura, and Y. Wakabayashi, Nat. Commun. **4**, 2022 (2013).

[14] S. Nakatsuji, K. Kuga, K. Kimura, R. Satake, N. Katayama, E. Nishibori, H. Sawa, R. Ishii, M. Hagiwara, F. Bridges, T. U. Ito, W. Higemoto, Y. Karaki, M. Halim, A. A. Nugroho, J. A. Rodriguez-Rivera, M. A. Green, and C. Broholm, Science **336**, 559 (2012).

[15] G. Khaliullin and S. Maekawa, Phys. Rev. Lett. **85**, 3950 (2000).

[16] G. Khaliullin and S. Okamoto, Phys. Rev. Lett. **89**, 167201 (2002).

[17] H. D. Zhou, B. S. Conner, L. Balicas, and C. R. Wiebe, Phys. Rev. Lett. **99**, 136403 (2007).

[18] Y. Imai, I. Solovyev, and M. Imada, Phys. Rev. Lett. **95**, 176405 (2005).

[19] G. Jackeli and G. Khaliullin, Phys. Rev. Lett. **102**, 017205 (2009).

[20] Y. Maeno, H. Hashimoto, K. Yoshida, S. Nishizaki, T. Fujita, J. G. Bednorz, and F. Lichtenberg, Nature (London) **372**, 532 (1994).

[21] G. Cao, J. Bolivar, S. McCall, J. E. Crow, and R. P. Guertin, Phys. Rev. B **57**, R11039 (1998); D. Haskel, G. Fabbris, M. Zhernenkov, P. P. Kong, C. Q. Jin, G. Cao, and M. van Veenendaal, Phys. Rev. Lett. **109**, 027204 (2012); B. J. Kim, H. Ohsumi, T. Komesu, S. Sakai, T. Morita, H. Takagi, and T. Arima, Science **323**, 1329 (2009); J. W. Kim, Y. Choi, J. Kim, J. F. Mitchell, G. Jackeli, M. Daghofer, J. van den Brink, G. Khaliullin, and B. J. Kim, Phys. Rev. Lett. **109**, 037204 (2012).

[22] M. Imada, A. Fujimori, and Y. Tokura, Rev. Mod. Phys. **70**, 1039 (1998).

[23] D. Senff, P. Reutler, M. Braden, O. Friedt, D. Bruns, A. Cousson, F. Bourée, M. Merz, B. Büchner, and A. Revcolevschi,

Phys. Rev. B **71**, 024425 (2005); B. J. Sternlieb, J. P. Hill, U. C. Wildgruber, G. M. Luke, B. Nachumi, Y. Moritomo, and Y. Tokura, Phys. Rev. Lett. **76**, 2169 (1996); S. B. Wilkins, P. D. Spencer, P. D. Hatton, S. P. Collins, M. D. Roper, D. Prabhakaran, and A. T. Boothroyd, *ibid.* **91**, 167205 (2003); S. Larochelle, A. Mehta, N. Kaneko, P. K. Mang, A. F. Panchula, L. Zhou, J. Arthur, and M. Greven, *ibid.* **87**, 095502 (2001).

[24] S. Anissimova, D. Parshall, G. D. Gu, K. Marty, M. D. Lumsden, S. X. Chi, J. A. Fernandez, D. L. Abernathy, D. Lamago, J. M. Tranquada, and D. Reznik, Nat. Commun. **5**, 3467 (2014).

[25] J. M. Longo and P. M. Raccah, J. Solid. State. Chem. **6**, 526 (1973).

[26] J. E. Greedan and W. Gong, J. Alloy. Compd. **180**, 281 (1992).

[27] S. L. Dudarev, G. A. Botton, S. Y. Savrasov, C. J. Humphreys, and A. P. Sutton, Phys. Rev. B **57**, 1505 (1998).

[28] K. Aso, J. Phys. Soc. Jpn. **44**, 1083 (1978).

[29] N. Qureshi, H. Ulbrich, Y. Sidis, A. Cousson, and M. Braden, Phys. Rev. B **87**, 054433 (2013).

[30] Y. Moritomo, K. Higashi, K. Matsuda, and A. Nakamura, Phys. Rev. B **55**, R14725 (1997).

[31] J. Goodenough, N. F. Mott, M. Pouchard, G. Demazeau, and P. Hagenmul, Mater. Res. Bull. **8**, 647 (1973).

[32] X. Qiu, T. Proffen, J. F. Mitchell, and S. J. L. Billinge, Phys. Rev. Lett. **94**, 177203 (2005).

[33] W. Miiller, M. Christensen, A. Khan, N. Sharma, R. B. Macquart, M. Avdeev, G. J. McIntyre, R. O. Piltz, and C. D. Ling, Chem. Mater. **23**, 1315 (2011).

[34] G. Kresse and J. Hafner, Phys. Rev. B **47**, 558 (1993).

[35] G. Kresse and J. Furthmüller, Phys. Rev. B **54**, 11169 (1996).

[36] W. Brzezicki, J. Dziarmaga, and A. M. Oles, Phys. Rev. Lett. **109**, 237201 (2012).

[37] L. F. Feiner, A. M. Oles, and J. Zaanen, Phys. Rev. Lett. **78**, 2799 (1997).

[38] J. C. T. Lee, S. Yuan, S. Lal, Y. I. Joe, Y. Gan, S. Smadici, K. Finkelstein, Y. J. Feng, A. Rusydi, P. M. Goldbart, S. L. Cooper, and P. Abbamonte, Nat. Phys. **8**, 63 (2012).

[39] S. Yuan, M. Kim, J. T. Seeley, J. C. T. Lee, S. Lal, P. Abbamonte, and S. L. Cooper, Phys. Rev. Lett. **109**, 217402 (2012).

[40] H. D. Zhou, Y. J. Jo, J. F. Carpino, G. J. Munoz, C. R. Wiebe, J. G. Cheng, F. Rivadulla, and D. T. Adroja, Phys. Rev. B **81**, 212401 (2010).

[41] For review, *Heisenberg Colloquium on Glassy Dynamics*, edited by J. L. van Hemmen and I. Morgenstern, Lecture Notes in Physics Vol. 275 (Springer-Verlag, Berlin, 1986).